Landslides (2014) 11:81–91
DOI 10.1007/s10346-012-0372-2
Received: 10 July 2012
Accepted: 19 November 2012
Published online: 12 December 2012

Boštjan Pulko · Bojan Majes · Matjaž Mikoš

Reinforced concrete shafts for the structural mitigation of large deep-seated landslides: an experience from the Macesnik and the Slano blato landslides (Slovenia)

Abstract During the last decade, several rainfall-induced deep-seated large landslides with volumes of the order of 1 million m^3 were triggered in various locations in Slovenia (central Europe), each representing a serious threat to the nearby villages and traffic infrastructure and urging to be mitigated. The Macesnik landslide, triggered in 1989, and the Slano blato landslide, triggered in 2000, were the first two large landslides in Slovenia, where a combination of drainage and retaining works consisting of deep reinforced concrete (RC) shafts/wells was successfully used as a mitigation measure. This paper presents the field conditions and a brief history of the two landslides with emphasis on the design approach and method used for the stability analysis and the design of deep RC shafts/wells. In addition, the paper gives an insight into the problems associated with the execution of works and provides data about the behavior of the two landslides after drainage and retaining works were completed. The monitoring data show that the undertaken mitigation measures were efficient to improve the stability of both landslides and significantly reduce the risk.

Keywords Slope stability · Landslide mitigation · Reinforced concrete shafts · Drainage works · Structural design · Monitoring

Introduction

Mitigation of large, deep, and fast-moving landslides is a difficult engineering task, which requires a good understanding of the causes and mechanisms that lead to slope failure. According to the International Union of Geological Sciences (IUGS) Working Group on Landslides, the landslide mitigation process includes the choice of one or a combination of the following four principle measures: modification of slope geometry, drainage, retaining structures, and internal slope reinforcement (Popescu 2001). The key elements for the successful use of one or a combination of these measures are field investigations and measurements that must provide all information necessary to investigate the stability of slopes.

At the time when several large deep-seated landslides with volumes of the order of 1 million m^3 were triggered during heavy rainfall in Slovenia (central Europe), there was little local experience with such large landslides. It was obvious that the mitigation approach should follow the basic principles combined with experience gained in the rehabilitation of smaller in size but phenomenologically similar landslides. In the case of the Macesnik and the Slano blato landslides, the general approach to mitigation was based on the frequently used measures in the Alpine region. These measures include the construction of surface drainage system and subsurface drainage system by means of interceptor trench drains or drainage wells in order to slow down the landslide movements to the extent that allows the construction of retaining structures in the form of stabilizing piles, retaining walls, or large diameter cast-in-place piles/shafts (Corsini et al. 2006; Marcato et al. 2012). For the structural mitigation of the two landslides, deep reinforced concrete (RC) shafts/wells were selected in order to combine the restraining effect of stabilizing piles (Hong and Han 1996; Popescu and Schaefer 2008; Kang et al. 2009; Song et al. 2012) and the dewatering effect of deep bore wells (Marschallinger et al. 2009) in a single type of construction.

Once detailed field data are collected, the design process of structural mitigation of the landslide is governed by slope stability analysis and retaining structure design calculations by means of various analytical and numerical methods. Although some analytical methods enable the calculation of lateral forces on piles/shafts in soil undergoing lateral movement (Ito and Matsui 1975; Ito et al. 1982; Firat 2009) and can be used for the design, they usually require a separate uncoupled slope stability analysis based on the limit equilibrium method in order to incorporate the reaction exerted on the unstable soil by the piles/shafts. Due to the three-dimensional (3D) nature of the problem and the complicated interaction behavior between the shaft and the moving soil mass, some of these methods are reported to be unreliable (Ito et al. 1982; Firat 2009). This is one of the reasons why numerical methods such as two-dimensional (2D) or 3D Finite Element Method (FEM) are becoming a viable, but not widely applied, alternative (Ng et al. 2001; Liang and Zeng 2002; Liang and Yamin 2010) for the structural design and stability evaluation.

In this paper, a brief history of the Macesnik and the Slano blato landslides is presented, with the emphasis on the mitigation approach and structural design of RC shafts/wells by means of 3D finite element analysis, together with construction experiences and performance evaluation after the completion of mitigation works.

Field conditions and brief history of the Macesnik and the Slano blato landslides

The Macesnik landslide is located at 46°26′ N, 14°41′ E above the village of Solčava in N Slovenia near the border with Austria (Figs. 1 and 2). The landslide was triggered in 1989 and is more than 2,500 m long, up to 100 m wide, and, on average, 10 to 15 m deep with an estimated volume of the sliding mass about 2 million m^3. The active landslide lies within the fossil landslide that is up to 350 m wide and 50 m deep with the total volume estimated at 8 to 10 million m^3. The crown of the landslide is at an altitude of 1,360 m and the toe, where the landslide was stopped by a large rock outcrop, at 840 m asl. In the period between 2000 and 2004, the landslide movements in the most critical upper part of the landslide reached up to 50 cm/day with an average value of 15 cm/day. The detailed description of the landslide occurrence, together with the explanation of geological–geotechnical conditions and measures taken in the period between 2001 and 2004 for a stepwise mitigation of the Macesnik landslide was previously reported by Mikoš et al. (2005). The mitigation works, which consisted of

subsurface drainage works and retaining works with deep RC shafts/wells, were completed in 2006.

The same approach using drainage works and RC shafts, acting also as drainage wells, was applied on the Slano blato landslide, which is located at 45°54′ N 13°51′ E (Figs. 1 and 3) in the Eocene flysch region of western Slovenia. The landslide was first mentioned in 1887 with the occurrence of an earth flow destroying the main road in the valley about 2 km away. The landslide was thereafter remediated with a series of torrential check dams along the Grajšček stream. The landslide remained stable till November 2000, when during heavy rainfall, a large landslide of mud and debris was triggered, moved along the Grajšček stream at a speed of up to 100 m/day and threatened the village of Lokavec situated in the valley below. The history of the landslide and geological, hydrogeological, hydrological, and geotechnical conditions for the occurrence of the landslide have been reported by several authors (Kočevar and Ribičič 2002; Majes et al. 2002; Logar et al. 2005; Placer et al. 2008). The landslide is about 1,600 m long, 60 to 250 m wide, with a total sliding mass of about 900,000 m^3 located between 270 and 650 m asl. In 2001 and 2002, approximately 230,000 m^3 of accumulated debris material were removed from the area of a rockfill dam that was built about 300 m above the village as a part of protection measures, followed by surface and subsurface drainage works and a construction of three RC shafts/wells in 2004, with gradual construction of additional eight RC shafts that were completed in 2007.

Although the conditions for the occurrence of the two landslides are geologically different—the Slano blato landslide is conditioned by weathering of the flysch at the border of Triassic limestone and Eocene flysch and the Macesnik landslide by complex geological conditions at the junction of Carboniferous, Triassic, and Oligocene rocks—they have a lot in common. Both landslides can be categorized as rainfall-induced landslides, which can also behave as earth flows consisting of clayey/silty gravels with high percentage of fines (>30 %) of low plasticity (PI>30) (Logar et al. 2005; Fifer and Zupančič 2009). Both landslides are long and relatively shallow with variable slope inclination and cannot be stopped by a single retaining structure. Thus, a similar design approach was adopted in the selection and design of mitigation measures for both landslides.

Evaluation of mitigation measures

In cases when rainfall-induced landslides are active, any execution of restraining work is a difficult, if not impossible, engineering task. It is of utmost importance that the restraining measures are designed not only to efficiently restrain the sliding mass but also to allow safe construction, with the likelihood of damage during the construction process reduced to an acceptable level. There were at least three additional problems that confronted the design of retaining constructions for the Macesnik and the Slano blato landslides. The first is that under heavy rainfall, the soil above the sliding plane can turn into a viscous earth flow, where the use of conventional geotechnical methods and material models can hardly be implemented. The second problem was associated with the length of both landslides, irregularity of the geological profile in the longitudinal and transverse directions, and finally, in the change of the terrain slope along the landslides. The third problem is the length of both landslides as compared to the depth of the sliding surface. In such conditions, it is usually impossible to stabilize the landslide with one retaining structure at a single location. Therefore, in order to achieve the best effect on stabilization, the selection of retaining structure locations was extremely important.

In the case of the Macesnik landslide, it was evident that the narrowing of the landslide in the area of a pontoon bridge is an ideal place for the first retaining structure in order to assure stability of the upper part of the landslide (Fig. 2). For the stabilization of the middle part of the landslide, the second location was selected in the area where the landslide is twice crossed by the ruined panoramic road. The third possible location was considered in the lower part of the landslide above the rock outcrop as shown in Fig. 4.

For the Slano blato landslide, the shaft location (see Fig. 3) was selected on the basis of observed sliding mechanism and professional judgment that is necessary to retain the sliding mass in the upper part of the landslide and prevent slippage of large quantities of weathered material along the Grajšček stream and to reduce progressive spreading of the landslide in the uphill direction. Considering the geology,

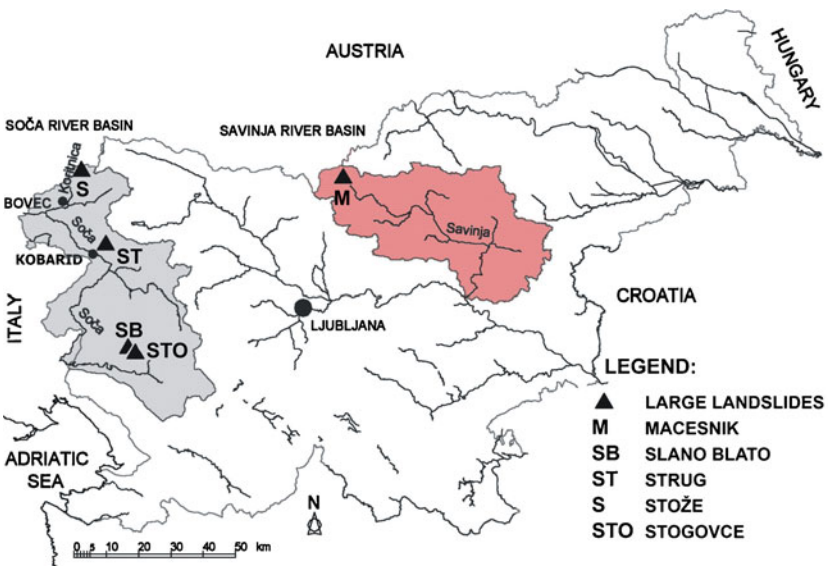

Fig. 1 Locations of the five large landslides in Slovenia

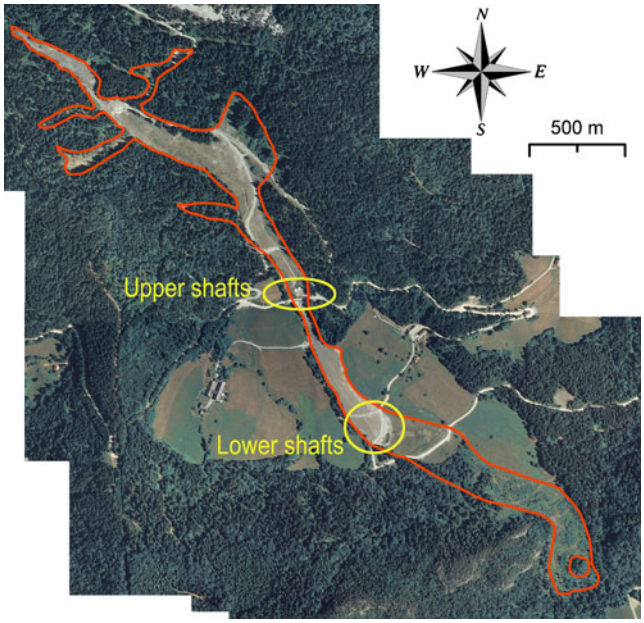

Fig. 2 Aerial view of the Macesnik landslide in 2005

size, and dynamics of the two landslides, the surface and subsurface drainage works (surface drainage and trench drains) were indispensable and were able to slow down the two landslides and enable the execution of restraining works.

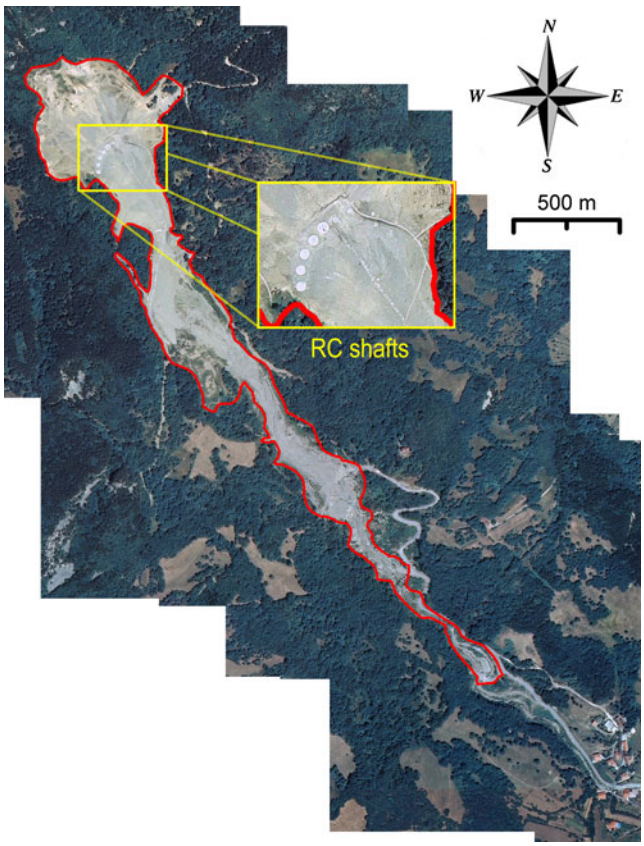

Fig. 3 Aerial view of the Slano blato landslide in 2006

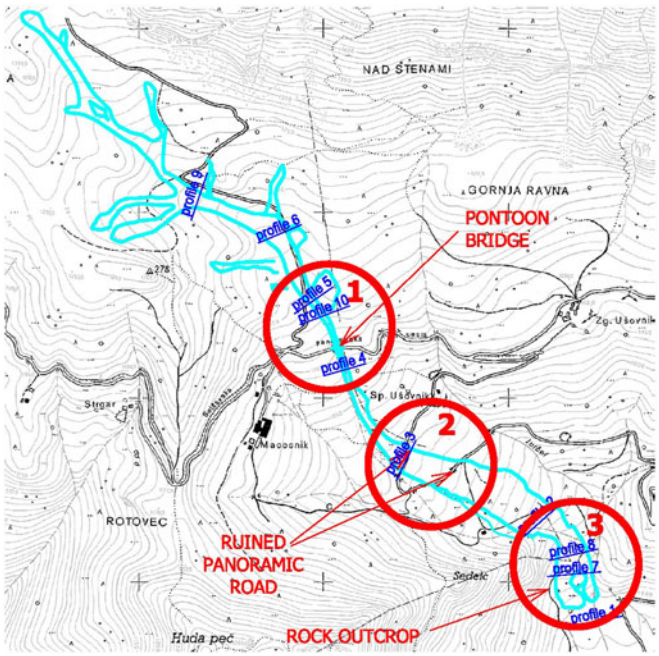

Fig. 4 Map of the Macesnik landslide with marked areas for the construction of retaining structures (from Mikoš et al. 2005)

The RC shafts (Fig. 5) were designed to provide stabilizing and dewatering effect on the sliding mass. The primary lining of the shaft consists of up to 30 cm thick and 1 m high reinforced cast in place concrete rings with an internal diameter of 5 m, which were connected in the vertical direction and separated from the sliding mass with an outer layer of drainage geotextile. With gradual deepening of the well, the rings were adequately perforated to allow the infiltration of the water and, if necessary, reinforced with steel wire mesh/ribs and up to 10 cm of shotcrete in order to sustain the loads of the sliding mass during the construction. In the stable base, additional polyethylene high-density (PEHD) drainage tubes (Φ125 mm) were installed at vertical distances of 3 m with a discharge into the interior of the well.

After reaching the final depth of the shaft/well, up to 4 m thick RC base plate was constructed, followed by the execution of the RC secondary lining with a thickness of 80 cm, which was designed to sustain the full force of sliding mass with prescribed factor of safety according to Eurocode standards. Finally, the shafts were interconnected with drainage pipes and a sewer pipe with a diameter of 160 mm was drilled by using horizontal directional drilling technology from the deepest well to the terrain surface and connected to the main drainage channel. In the case of the Slano blato landslide, additional vertical drainage pipes were installed through the base plate of the shaft to collect water from the flysch layers and acting as pressure relief pipes. The details dealing with the design and execution of mitigation works on both landslides are given below for each landslide separately.

Design and execution of mitigation works

Macesnik landslide

The stability analysis of the Macesnik landslide and shaft design calculations were performed using 3D FEM with the adoption of elastoplastic constitutive model for the displaced material and for

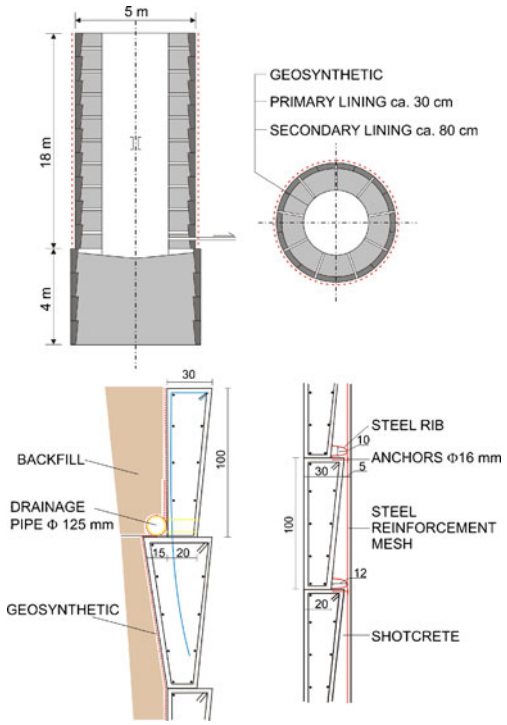

Fig. 5 Vertical cross-section of the reinforced concrete shaft

the underlying layers and bedrock. Commercial FEM software Plaxis 3D Foundation (Brinkgreve and Broere 2004) was used for the analysis.

Elastoplastic model with isotropic hardening, also known as hardening soil (HS) model (Schanz et al. 1999), was used to model the soils and bedrock. The HS model is an advanced soil model with stress-dependent stiffness and allows for plastic straining due to primary compression and deviatoric loading and distinguishes between primary loading and elastic unloading/reloading. The failure is defined according to the Mohr–Coulomb criterion. Soil stiffness and strength parameters for the numerical analysis were determined on the basis of laboratory tests and are shown in Table 1.

For computational reasons, it was not possible to model the entire landslide. Thus, only appropriate sections with the proposed shafts were considered in the analysis. The design approach and method of analysis for all three locations were the same as described below for the case of shafts at the uppermost location of the landslide (Fig. 2). For this section of the landslide, the total length of numerical model in the slope direction was determined according to the expected effect of the shafts on the landslide stability and set to 200 m, extending 70 m above and 130 m below the planned shafts as shown in Fig. 6a, where the finite element mesh of the model with activated shaft elements is depicted. The width of the computational model (30 m) was consistent with the landslide width at the proposed shaft location. Other geometric characteristics of the computational model were set according to the transverse and longitudinal profiles of the terrain, geological data, and geometry/symmetry of the planned constructions.

Two RC shafts, both 22 m deep and 5 m in diameter, were positioned 10 m apart and modeled as concrete elastic shells with primary lining thickness of 30 cm and final wall thickness of 110 cm. Young modulus of the concrete (class C25/30) was set according to Eurocode 2 (EN 1992-1-1:2004) E_c=31 GPa.

The design calculation was carried out on the basis of back analysis of the landslide, which is commonly used to estimate the shear strength of the sliding surface and reproduce the actual displacement of the sliding mass (Ishii et al. 2001). Numerical modeling was conducted in the following steps:

- Calculation of the initial stress state;
- Back analysis of the landslide;
- Calculation of loads on the primary shaft lining at various construction stages; and
- Calculation of total loads on the primary and secondary shaft linings for the final state of construction and for the critical state under the worst possible conditions.

It should be noted that the dynamic effects due to the speed of the landslide movement were not considered in the analyses because of the successful completion of drainage measures, which reduced the displacement rates to an acceptable level.

The initial stress state in the model was generated for the prefailure state with a low ground water level approximately 5 m below the terrain surface, as measured during the dry periods after the surface drainage system was executed. Numerically, it was done

Table 1 Basic soil/rock stiffness and strength parameters

Soil/rock	Symbol	Unit	Sliding mass	Fossil landslide	Bedrock
Unit weight	γ	(kN/m^3)	21	22	24
Cohesion	c'	(kPa)	0	5	200
Friction angle	ϕ'	(°)	32	36	40
Angle of dilatancy	ψ	(°)	0	0	0
Secant stiffness modulus	E_{50}^{ref}	(MPa)	5	20	120
Tangent stiffness modulus	E_{oed}^{ref}	(MPa)	5	25	120
Unloading/reloading stiffness modulus	E_{ur}^{ref}	(MPa)	15	60	360
Reference stress	p^{ref}	(kPa)	100	100	100
Poisson's ratio for unloading/reloading	ν_{ur}	–	0.2	0.2	0.2
Stiffness parameter	m	–	0.5	0.5	0.5

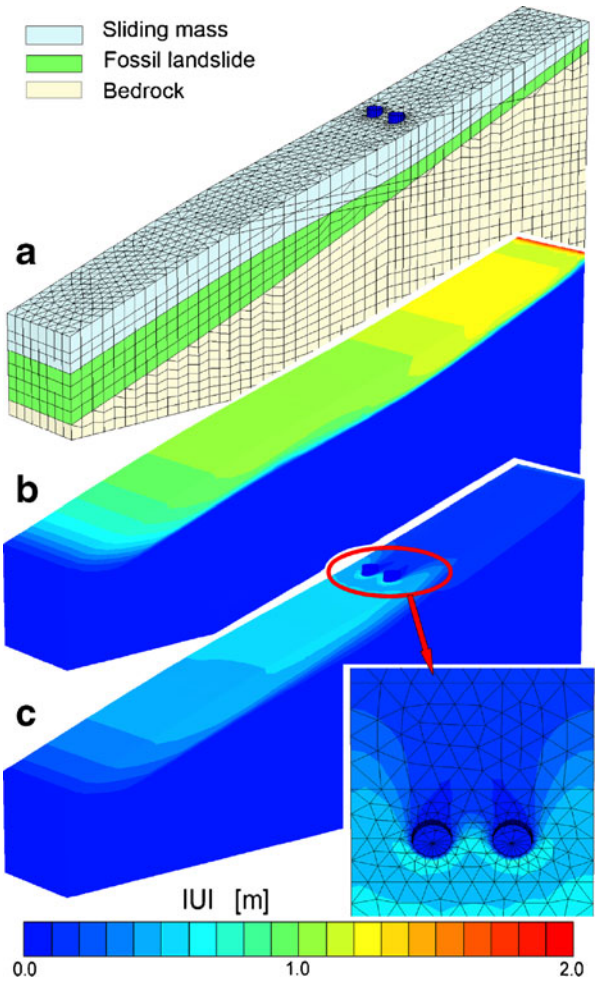

Fig. 6 Finite element mesh with activated structural elements (**a**), failure mechanism at the state of nonconvergence (back analysis) with deactivated structural elements (**b**) and calculated displacements for the final state plotted as contour shadings of displacements with a detailed view of the calculated displacements around shafts (**c**)

in the initial phase of the finite element calculation in which soil weight and water pressures were applied by means of gravity loading.

In the next phase, the back analysis of the landslide was performed. In order to numerically simulate on-site conditions and behavior of the landslide, the ground water level was gradually "raised" from the initial state (−5 m). Through iterative computation, the model was brought to a state of nonconvergence when the water level was just below the surface of the terrain (−0.1 m). As the numerical procedure fails due to soil plastification, it generates large displacements, which indicate the sliding mechanism (Fig. 6b). The results of back analysis were consistent with the sliding mechanism, depth of the sliding zone, and field conditions as observed on site.

As it was realized that in dry periods, the surface drainage works are sufficient to stabilize the landslide to the extent that it allows the construction of shafts, the primary shaft lining, composed of segmental cast-in-place RC rings, was designed to sustain the loads during the construction when the landslide is dormant. The negative experience at the Slano blato landslide showed that such an approach was too risky, leading to a change in the design and construction method as described in the next section.

Although the shafts were designed also as drainage wells, the drainage effect was not considered in the critical analysis in order to get the characteristic shaft loads for the worst-case scenario (WCS), e.g., failure of the subsurface sewer pipe and drainage system. Therefore, the loads on the shafts (primary and secondary linings) were calculated with the numerical simulation of groundwater level rise to the model surface. Figure 6c shows the calculated displacements plotted as contour shadings for the WCS, with clearly visible arching effect behind the shafts and sliding of the soil mass along the shaft wall with final displacement reaching up to 0.5 m, which is sufficient to achieve full load transfer of the active landslide upon the shafts. The calculated shaft displacements with maximum value reaching up to 56 mm are shown in Fig 7. Figure 8 shows the most important internal axial forces, bending moments, and shear forces in the shaft wall plotted as contour shadings, with the notation according to the scheme of internal forces as shown in Fig. 9.

The calculation of safety factor for the WCS by using shear strength reduction method (Zienkiewicz et al. 1975; Dawson et al. 1999) showed that the impact of shafts on the stability of the slope below the shafts was marginal, which did not allow the calculation of the design loads at safety factor of 1.25 required by Eurocode 7 (EN 1997–1:2004). Therefore, the design values of shaft internal forces (axial forces ($N_{1;d}$, $N_{2;d}$), bending moments ($M_{11;d}$, $M_{22;d}$, $M_{12;d}$) and

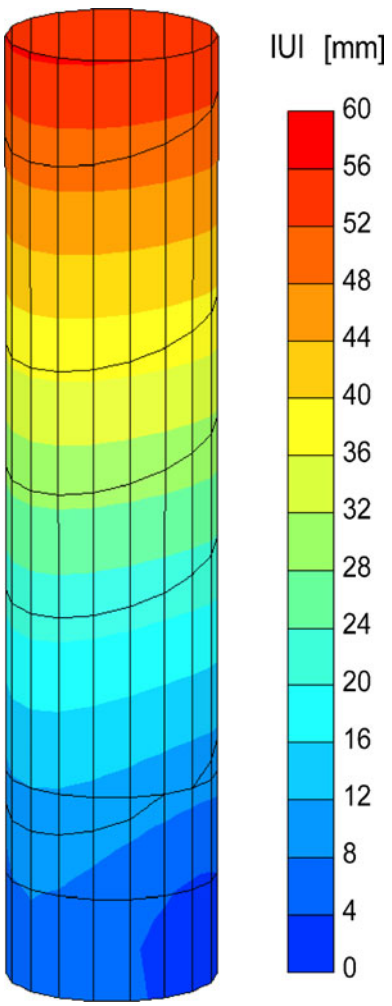

Fig. 7 Contour shadings of maximum shaft displacements

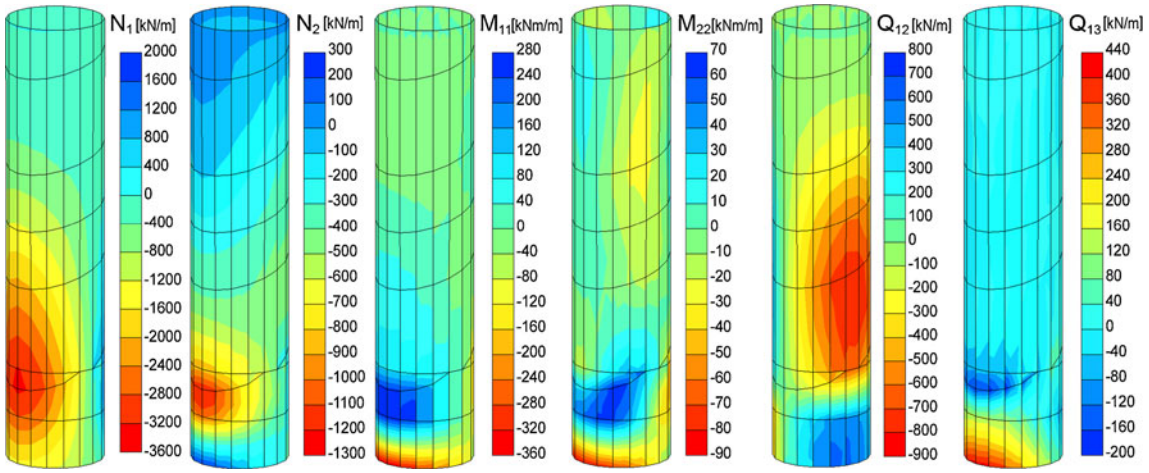

Fig. 8 Contour shadings of the characteristic internal axial forces, bending moments, and shear forces in the shaft wall

shear forces ($Q_{12;d}$, $Q_{13;d}$, $Q_{23;d}$) for the WCS were calculated according to Eurocode 7 (EN 1997–1:2004), which allows the multiplication of the effects of actions shown in Fig. 8 (characteristic values of shaft loads), with the partial safety factor of 1.35.

Additional analyses showed that the downslope stability could only be ensured, if the ground water level is kept −3 to −3.5 m below the terrain surface. Therefore, the construction of 3 to 4 m deep drainage trench along the slope was proposed and executed after the completion of the shafts (Fig. 12). The analysis taking into account the lowering of ground water level and a safety factor of 1.25(case herein named LWL) yielded comparable distribution but, in general, less extreme design values of shaft internal forces than the analysis for the WCS. Extreme design values of shaft internal forces for WCS and LWL analyses are shown in bold text in Table 2 together with accompanying values of internal forces in the same cross-section.

Although the internal forces were calculated by taking into account the shaft wall thickness of 110 cm, the 80 cm thick secondary lining was designed to sustain the whole (100 %) load induced by the sliding mass. The primary lining was designed to sustain only the loads during the construction. Figure 10 shows the ultimate resistance surface of the secondary lining and ultimate design loads for WCS at the $N_1 - M_{11}$ diagram according to Eurocode 2 standard (EN 1992-1-1:2004).

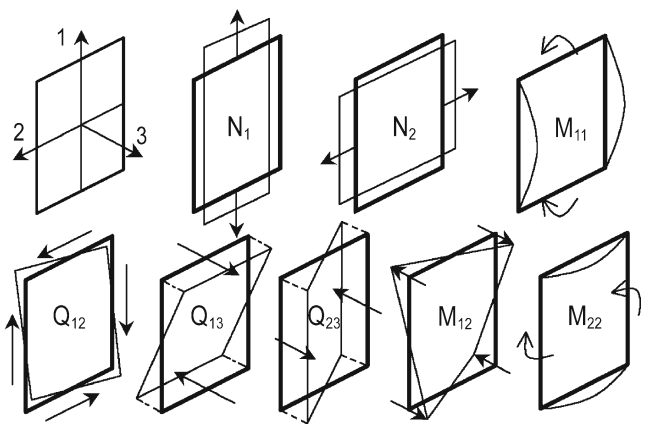

Fig. 9 Scheme and notation of internal forces

The construction of the first two shafts, each about 22 m deep and 5.4 m in external diameter, began in autumn 2004, after three drainage trenches (250 m long, up to 8 m deep) had been executed in order to reduce unacceptably high displacement rates up to 50 cm/day in the 800 m long uppermost section of the landslide. The shafts are situated in the area just above the pontoon bridge and were completed in spring 2005, followed by the construction of the drainage trench on the steeper slope below (Figs. 11 and 12). In 2006, the mitigation works were completed with the construction of two additional deep RC shafts in the middle area of the landslide, where it is twice crossed by the panoramic road. No further measures were taken in the lower part of the landslides as planned previously (Mikoš et al. 2005).

Slano blato landslide

A similar approach as for the Macesnik landslide was used to design shafts for the Slano blato landslide, taking into account the relevant geological, hydrological, and geotechnical data (Majes et al. 2002; Fifer and Zupančič 2009). Initially, five shafts at mutual distances of 15 m, each 5.4 m in diameter and 20 m deep, were planned to be executed in the central part of the landslide, with gradual construction of additional shafts towards the edges of the landslide, if it proved to be necessary. Since the back analysis with the numerical consideration of water level on the ground surface was insufficient to create sliding mechanism as observed on site, additional artesian water pressure (50 kPa) at the contact between the sliding mass and flysch base was considered in the analysis (Fig. 13), confirming the field observations that an important influx of water to the sliding mass also came from a lower flysch layer (Logar et al. 2005; Placer et al. 2008). In order to minimize the negative effect of these pressures, additional vertical drainage pipes were planned to be installed through the concrete shaft base to work as pressure relief pipes.

The construction of three central shafts started in autumn 2004. After intense rainfall in October 2004 (monthly rainfall accumulation 377 mm, of which 118 mm between October 29 and 31), a large amount of water and strong inflow of ground water from the flysch rock into the area of shafts, which were under construction and had not yet penetrated into stable bedrock, caused excessive earth movements between November 1 and 2. In just 2 days, the shafts were displaced by nearly 20 m (Figs. 13 and 14). The primary lining of one shaft, which was at that time excavated to the depth of 6 m, was

Table 2 Extreme and accompanying design internal forces for WCS and LWL case (LWL values in brackets)

	$N_{1;d}$ (kN/m)	$N_{2;d}$ (kN/m)	$M_{11;d}$ (kNm/m)	$M_{22;d}$ (kNm/m)	$M_{12;d}$ (kNm/m)	$Q_{12;d}$ (kN/m)	$Q_{13;d}$ (kN/m)	$Q_{23;d}$ (kN/m)
$N_{1;d\_max}$ (kN/m)	**2,696 (2,627)**	−63 (−55)]	−278 (−249)	−57 (−40)	3 (3)	−14 (45)	7 (7)	7 (18)
$N_{1;d\_min}$ (kN/m)	**−4,433 (−4,238)**	−1,596 (−1,377)	327 (342)	31 (64)	28 (37)	−3 (13)	−251 (−311)	−274 (−234)
$N_{2;d\_max}$ (kN/m)	−2,055 (−1,687)	**296 (341)**	−467 (−388)	−111 (−91)	−27 (−20)	−128 (−117)	567 (477)	61 (61)
$N_{2;d\_min}$ (kN/m)	−4,432 (−4,229)	**−1,692 (−1,453)**	365 (390)	43 (80)	28 (37)	−23 (−23)	−200 (−186)	−266 (−215)
$M_{11;d\_max}$ (kNm/m)	−2,005 (−1,638)	−1,131 (−1,351)	**394 (405)**	86 (95)	16 (30)	375 (−192)	134 (−135)	−201 (−220)
$M_{11;d\_min}$ (kNm/m)	−2,005 (−1,638)	257 (309)	**−477 (−400)**	−113 (−94)	20 (12)	−212 (−191)	540 (441)	−69 (−73)
$M_{22;d\_max}$ (kNm/m)	−3,803 (−4,054)	−1,297 (−1,351)	362 (405)	**101 (95)**	18 (30)	−311 (−192)	−96 (−135)	−215 (−220)
$M_{22;d\_min}$ (kNm/m)	−2,005 (−1,638)	257 (309)	−477 (−400)	**−113 (−94)**	20 (12)	−212 (−191)	540 (441)	−69 (73)
$M_{12;d\_max}$ (kNm/m)	751 (−4,030)	−320 (−1,301)	−219 (312)	−30 (59)	**41 (42)**	−829 (159)	−53 (−330)	62 (−246)
$M_{12;d\_min}$ (kNm/m)	−3,731 (−4,058)	−1,234 (−1,272)	261 (325)	93 (81)	**−36 (−42)**	−275 (−159)	−284 (−334)	277 (266)
$\lvert Q_{12;d\_max}\rvert$ (kN/m)	−325 (−396)	−602 (−359)	9 (13)	−7 (9)	8 (−6)	**1,149 (1,053)**	−31 (−21)	−80 (61)
$\lvert Q_{13;d\_max}\rvert$ (kN/m)	−1,962 (−1,687)	263 (341)	−475 (−338)	−107 (−91)	−23 (−20)	225 (−117)	**570 (477)**	73 (61)
$\lvert Q_{23;d\_max}\rvert$ (kN/m)	−4,275 (−4,058)	−1,481 (−1,272)	323 (325)	61 (81)	−32 (−42)	−84 (−159)	−277 (−334)	**328 (266)**

Extreme design values of shaft internal forces for WCS and LWL analyses are shown in bold together with accompanying values of internal forces in the same cross-section

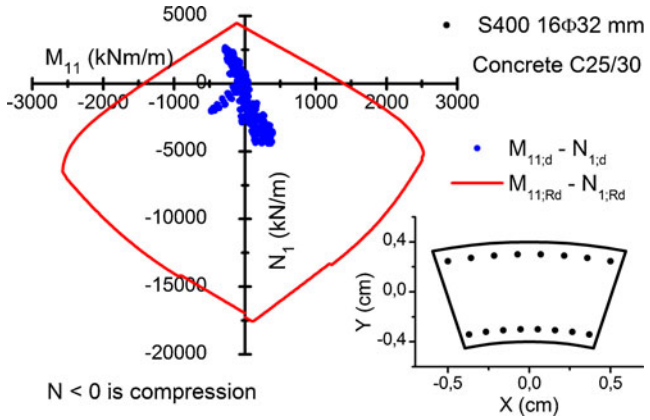

Fig. 10 Ultimate resistance surface of the secondary lining and ultimate design loads (N_1–M_{11} diagram) with a scheme of longitudinal reinforcement in the secondary lining of the shafts

damaged beyond repair, while two others suffered only minor damage and were later completed at the displaced location. Although not reaching the stable bedrock and severely displaced, the shafts were able to collect a large amount of water, which was pumped out and discharged from the area. In the period between October 31 and November 6, each shaft was able to collect about 200 to 240 m^3 of water per day (2.3–2.8 l/s). The decreased displacement that took place in the next few days was mainly due to successful drainage of the sliding mass. This event confirmed the hydrological forecast that during intense rainfall each well should be able to collect about 2.8 l/s of water from the most permeable top 4 m of the sliding mass and additional 1 l/s from the soil below (Prestor et al. 2004).

To speed up the construction and reduce the risk of potential damage to shafts during their construction, the design of the shaft was changed. The segmental concrete rings (primary lining) were replaced with eight bored RC piles with diameters of 150 cm, which were then on their tops connected with a 1.5 m high RC ring beam. The centers of piles are on circles with a diameter of 6.5 m to allow the final construction of the secondary RC lining with the inner diameter of 4.2 m. The spatial scheme of the shaft with its cross-section is shown in Fig. 15. The damaged shaft was replaced in 2005 and four additional shafts were constructed on the right-hand side of the landslide. By the end of 2007, when mitigation works on the upper part of the landslide were completed, four additional deep shafts were executed on the left-hand side of the landslide. The shafts

Fig. 11 Interior of the shaft during the execution of the secondary lining

Fig. 12 Construction of the drainage trench in the middle section of the Macesnik landslide

Fig. 14 Primary lining of the shaft at the Slano blato landslide during construction. The *photo* shows the drainage ability of the shafts/wells

were positioned in semicircular form to act as an arch and transfer the loads from the retained soil laterally into to the stable ground.

Monitoring and performance evaluation

The Macesnik and the Slano blato landslides are typical examples where conventional methods for monitoring displacement or pore water pressures (e.g., inclinometers and piezometers) can hardly be implemented due to excessive and rapid movements of the sliding mass. In order to evaluate the performance of the applied mitigation measures, one had to rely on other methods of monitoring, which contained conventional geodetic measurements of displacements, Global Positioning System (GPS) based displacement measurements, advanced geodetic measurements including ground and air Light Detection And Ranging (LIDAR) measurements, weather monitoring (rainfall, temperature, wind, and sunshine duration), monitoring of ground water levels in the soil/wells, and soil matric suction measurements.

As both landslides are rainfall induced, the amount of precipitation has a major influence on the landslide activity. Thus, it is of great importance (Hong et al. 2005) to assess the influence of rainfall on landslide movements and, consequently, to assess the impact of the measures implemented.

Macesnik landslide

As shown in Fig. 16, where local daily, monthly, and cumulative yearly precipitation measured in the rainfall gauging station in the village of Solčava are depicted (1 km away from the toe of the Macesnik landslide), the precipitation in 2006 was slightly lower than in previous years but at the same level in the subsequent years with a series of rainfall events that would normally trigger the landslide.

The intense movements up to 50 cm/day at the Macesnik landslide in the period between 2000 and 2004 have rapidly declined after the completion of mitigation works in the upper part of the landslide in September 2004. Figure 17 shows the absolute displacements and displacement rates in measuring cross-sections on the Macesnik landslide for the period from 8 September 2004 to 29 September 2005. The displacement rates were further reduced when drainage works and retaining works had been completed in the middle section of the landslide in 2006. The maximum recorded

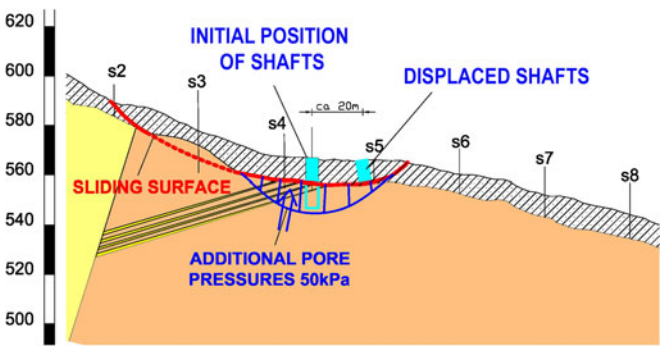

Fig. 13 Cross-section of the Slano blato landslide

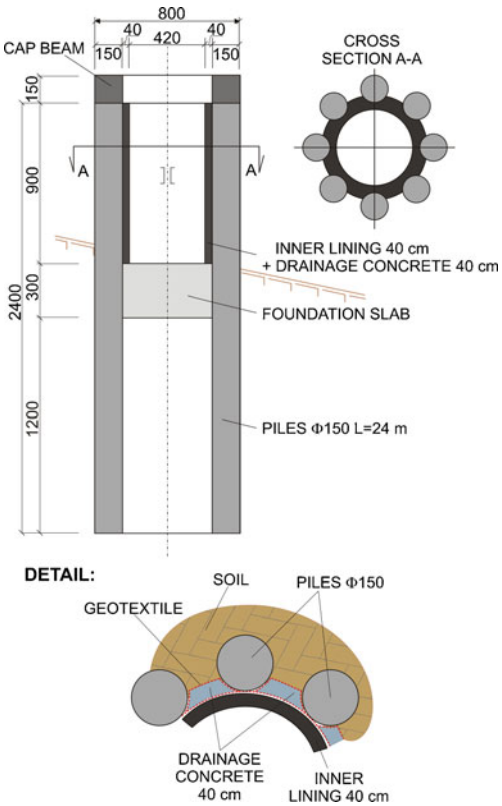

Fig. 15 Spatial scheme with *vertical* and *horizontal cross-section* of the modified design

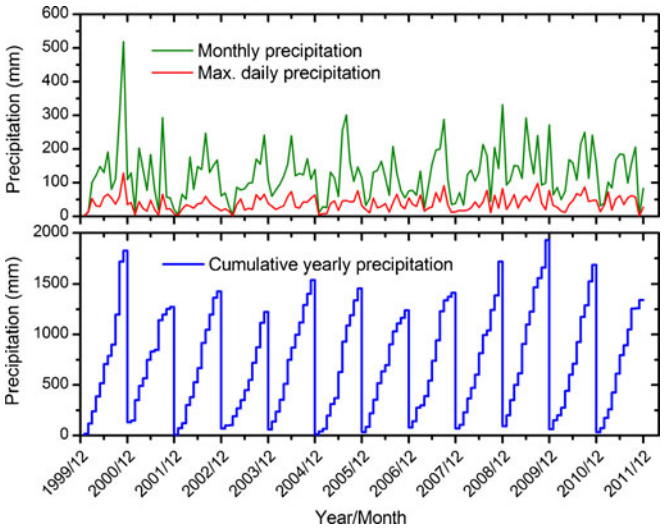

Fig. 16 Rainfall data measured in the village of Solčava—Macesnik landslide (2000–2012)

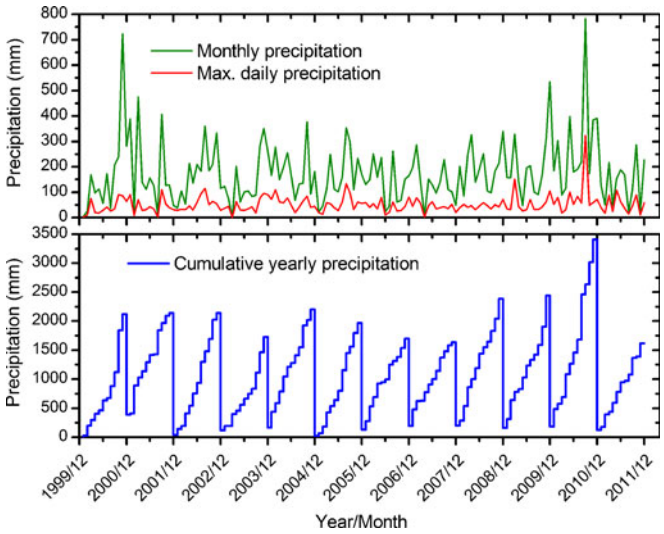

Fig. 18 Rainfall data measured in the village of Otlica—Slano blato landslide (2000–2012)

displacement of the upper shafts was 36 mm, which is about 63 % of the predicted displacement for the WCS (56 mm). From 2006 to date, no landslide activity has been reported in the upper and middle sections of the landslide where mitigation measures were executed as planned.

Slano blato landslide

The precipitation data for the Slano blato landslide (Fig. 18) were taken at a rainfall gauging station in the village of Otlica situated approximately 3.8 km east of the landslide. The landslide was triggered in November 2000 with a monthly rainfall amount of 723 mm and daily maximum 86 mm. A series of events causing serious advancements of the sliding mass in the subsequent years showed good correlation with the amount of precipitation. Both peaks observed in March and September 2001 (Fig. 18) with monthly rainfall over 400 mm and daily maximum over 70 mm were followed by significant earth flow advancements. The next triggering event was in November 2004 (377 mm/month and 83.6 mm/day), when the shafts were severely displaced. Based on these events, it was estimated that monthly rainfall over 350 mm accompanied with the daily maximum of about 70 mm of rainfall is sufficient to trigger the landslide.

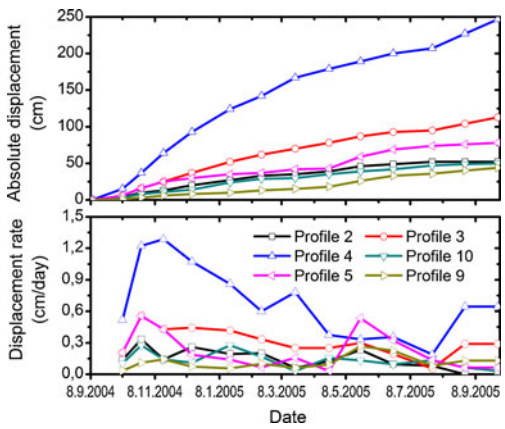

Fig. 17 Absolute displacements and displacement rates in measuring cross-sections on the Macesnik landslide (see Fig. 4 for the position of cross-sections)

As seen from the rainfall data measured in the rainfall gauging station in the village of Otlica (3.8 km away from the Slano blato landslide) in Fig. 18, 2005, and especially 2006 and 2007 were rather dry years. However, after 2007, when mitigation works at the Slano blato landslide were completed, a number of critical rainfall events have happened, causing some local earth movements at the main scarp but have not been able to trigger the landslide. The final test of the executed measures was conducted during heavy rainfall in September 2010, when the record with 498 mm of rainfall in 48 h between 17 and 19 September was recorded and large landslide Stogovce located nearby was triggered (Petkovšek et al. 2011). The impact on the Slano blato landslide was marginal, as it remained stable and no damage at the 11 executed RC shafts and drainage channels was observed, as can be seen from the aerial view of the upper part of the remediated landslide (Fig. 19). In 2007, after the completion of the shafts, ground LIDAR measurements were taken in order to get better insight into the behavior of the upper part of the landslide, where occasional local earth movements were still observed during heavy rainfall.

Figure 20 shows a 3D view of the upper part of the landslide as recorded by ground LIDAR measurements in 2007 and Fig. 21, the difference in the terrain height recorded in February and October 2007. The colder colors (blue) show the areas where the terrain was lower in October 2007 than in February 2007, while warmer colors (red) show the opposite. From the data (Fig. 21), it is evident that some local sliding of the soil occurred in the upper part of the landslide, which leads to the change of terrain level within −3 m and +4 m. The terrain around the shafts remained stable, although some ground subsidence (blue areas) can be detected above the shafts (due to the drainage) and in the area below the shafts, where some erosion and shallow earth slips were detected. The net volume of the soil mass, obtained as the difference in the terrain height, was found to be positive, which means that the terrain measured in October was, on average, higher than that measured in February 2007. This is most probably due to the accumulation of the material from the periphery of the observed area and flysch rock deterioration, although it could

Fig. 19 Aerial view of the upper part of the Slano blato landslide

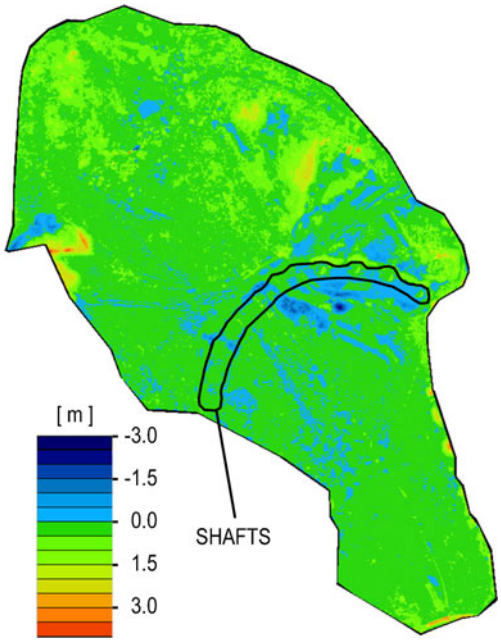

Fig. 21 Difference in the terrain height in the period from February 2007 to October 2007

also be due to the horizontal movements. Nevertheless, the calculated net volume confirms the ability of the applied stabilizing measures to successfully retain the earth mass in the upper area of the landslide.

Drainage ability of the shafts was observed by real-time measurements of the water levels in one of the wells and piezometer, which was placed about 10 m above the shafts in the stabilized ground. The data compared to the amount of daily precipitation are shown in Fig. 22. The groundwater level in the area above the shafts, which used to be at the terrain surface, has dropped by about 4 m and remains at that level regardless of the daily precipitation. The water level in the well shows a rapid increase immediately after heavy rainfall and rapid decrease thereafter. This indicates high drainage capacity of wells that exceeds the capacity of subsurface sewer pipes with a diameter of 160 mm. Consequently, shafts/wells act as temporary water detention storage. The data also show a successful reduction of the groundwater level in the shaft hinterland, which was not taken into account during the design and significantly contributes to the stability.

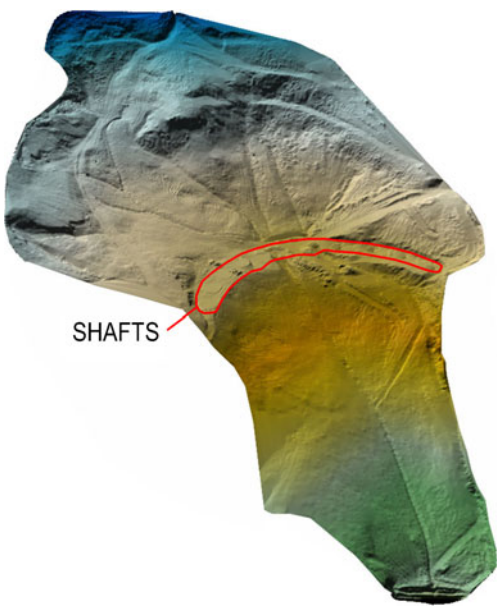

Fig. 20 3D view of the upper part of the Slano blato landslide (February 2007)

Conclusions

This study presents a case history of successful remediation of the Macesnik and the Slano blato landslides with a combination of drainage and retaining works with an emphasis on the design and execution of the RC shafts/wells. The simultaneous use of shafts and deep drainage works has proved to be an effective measure to increase the stability and reduce the landslide risk. Several years after the completion of RC shafts at the two landslides, the following conclusions can be drawn:

1. The study shows that initial geological and geotechnical surveys, together with an efficient monitoring system, have a decisive influence on the choice of mitigation measures. The locations for retaining constructions should be selected according to the size and speed of landslide movements, length of the landslide, irregularities in the geological profile in the

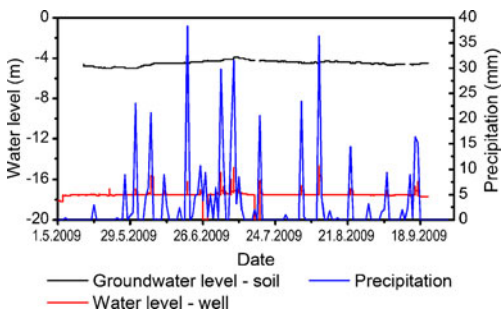

Fig. 22 Groundwater levels and precipitation data for the period between 1 May and 21 September 2009—Slano blato landslide

longitudinal and transverse directions, and change of the slope along the landslide.

2. In case of fast-moving landslides, the execution of drainage works is indispensable in order to slow down the landslide and to enable the execution of retaining works. In order to design appropriately a retaining construction, its execution must be taken into account in order to minimize the construction risk and to avoid damage during the construction.
3. The FEM has been applied for the design of deep RC shafts. The numerical analysis should be based on the back analysis of the landslide and consider all construction phases during and after the execution of works. Numerical simplifications are inevitable and therefore, the impact on the final results should be carefully examined in the design process.
4. RC shafts with twofold function of restraining and draining have proved to be an effective measure for the structural mitigation of large and fast-moving landslides such as the Macesnik and the Slano blato landslides. Both landslides were efficiently slowed down. The shaft behavior was found consistent and in good agreement with the design expectations. The measured shaft displacements do not exceed the predicted values and no structural damage was observed during the extreme rainfall events after the completion of works.
5. The measurements of the groundwater level in the vicinity of the shafts have proved the high drainage capacity and successful reduction of the groundwater level, which adds considerably to the stability of both landslides.
6. According to the monitoring data, the mitigation measures at both landslides can be assessed as effective in preventing the reoccurrence of large-scale sliding under heavy rainfall, although the emergence of minor earth movements is still possible.

Acknowledgments

This research was financially supported by the Slovenian Research Agency, grant No. P2-0180 "Hydromechanics, hydraulics and geotechnics." The precipitation data were made available by the Environmental Agency of Slovenia. The authors would like to thank Mr. Igor Benko, the Commander of the Civil Protection of the Ajdovščina Municipality, for providing monitoring data on the behavior of the Slano blato landslide. The authors would also like to acknowledge the editor and reviewers for their constructive comments that improved the paper.

References

Brinkgreve RBJ, Broere W (2004) Plaxis 3D foundation—version 1. Plaxis bv, Netherlands

Corsini A, Borgatti G, De Simone N, Sartini G, Truffelli G (2006) Investigation and monitoring in support structural mitigation of large slow moving landslides: an example from Ca' Lita (Northern Apennines, Reggio Emilia, Italy). Nat Hazards Earth Syst Sci 6:55–61

Dawson EM, Roth WH, Drescher A (1999) Slope stability analysis by strength reduction. Geotechnique 49(6):835–840

EN 1992-1-1:2004 Eurocode 2: design of concrete structures: general rules and rules for buildings

EN 1997–1:2004 Eurocode 7: geotechnical design: general rules

Fifer BK, Zupančič VA (2009) Site and laboratory investigation of the Slano blato landslide. Eng Geol 105(3):171–185

Firat S (2009) Stability analysis of pile slope system. Sci Res Essay 4(9):842–852

Hong WP, Han JG (1996) The behavior of stabilizing piles installed in slopes. Proceedings of the 7th International Symposium on Landslides, Trondheim. Norway 3:1700–1714

Hong Y, Hiura H, Shino K, Sassa K, Fukuoka H (2005) Quantitative assessment on the influence of heavy rainfall on the crystalline schist landslide by monitoring system—case study on Zentoku landslide, Japan. Landslides 2(1):31–41

Ishii Y, Keiichi O, Kuraoka S, Tsunaki R (2001) Evaluation of slope stability by finite element method using observed displacement of landslide. Landslides 14. doi:10.1007/s10346-011-0303-7

Ito T, Matsui Z (1975) Methods to estimate lateral force acting on stabilizing piles. Soils Found 18(2):43–59

Ito T, Matsui T, Hong WY (1982) Extended design methods for multi row stabilizing piles against landslide. Soils Found 220(1):1–13

Kang GC, Song YS, Kim TH (2009) Behaviour and stability of a large cut slope considering reinforcement stages. Landslides 6(3):63–272. doi:10.1007/s10346-009-0164-5

Kočevar M, Ribičič M (2002) Geological, hydrogeological and geomechanical investigation of Slano blato landslide. Geologija 45(2):427–432. doi:10.5474/geologija.2002.043 (in Slovene)

Liang RY, Yamin M (2010) Three dimensional finite element study of arching behaviour in slope/drilled shafts system. Int J Numer Anal Methods Geomech 34:1157–1168

Liang RY, Zeng S (2002) Numerical study of soil arching in drilled shafts for slope stabilization. Soils Found 42(2):83–92

Logar J, Fifer BK, Kočevar M, Mikoš M, Ribičič M, Majes B (2005) History and present state of the Slano blato landslide. Nat Hazard Earth Syst Sci 5:447–457

Majes B, Petkovšek A, Logar J (2002) The comparison of material properties of debris flows from Stože, Slano blato and Strug landslides. Geologija 45(2):457–463. doi:10.5474/geologija.2002.048

Marcato G, Mantovani M, Pasuto A, Zabuski L, Borgatti L (2012) Monitoring, numerical modeling and hazard mitigation of the Moscardo landslide (Eastern Italian Alps). Eng Geol 128:95–107

Marschallinger R, Eichkitz C, Gruber H, Heibl K (2009) The Gschliefgraben landslide (Austria): a remediation approach involving torrent and avalanche control, geology, geophysics, geotechnics and geoinformatics. Austrian J Earth Sci 102102(2):36–51

Mikoš M, Fazarinc R, Pulko B, Petkovšek A, Majes B (2005) Stepwise mitigation of the Macesnik landslide, N Slovenia. Nat Hazard Earth Syst Sci 5:948–958

Ng CWW, Zhang LM, Ho KKS (2001) Influence of laterally loaded sleeved piles and pile groups on slope stability. Can Geotech J 38(3):353–566

Petkovšek A, Fazarinc R, Kočevar M, Maček M, Majes B, Mikoš M (2011) The Stogovce landslide in SW Slovenia triggered during the September 2010 extreme rainfall event. Landslides 8(4):499–506. doi:10.1007/s10346-011-0270-z

Placer L, Jež J, Atanackov J (2008) Structural aspect on the Slano blato landslide (Slovenia). Geologija 51(2):229–234. doi:10.5475/geologija.2008.023 (in Slovene)

Popescu ME (2001) A suggested method for reporting landslide remedial measures. IAEG Bull 60(1):69–74

Popescu ME, Schaefer VR (2008) Landslide stabilizing piles: a design based on the results of slope failure back analysis. Proceedings of the 10th International Symposium on Landslides and Engineered Slopes, Xi'an, China, pp 1787–1793. doi:10.1201/9780203885284-c247

Prestor J, Hoetzl M, Kočevar M (2004) Report on the hydrological conditions at the Slano blato landslide during the construction of drainage wells 03.11.2004. Geological Survey of Slovenia and Geoinženiring d.o.o., Interim report, pp 15 (in Slovene)

Schanz T, Vermeer PA, Bonnier PG (1999) The hardening-soil model: formulation and verification. Beyond 2000 in Computational Geotechnics. Balkema, Rotterdam, pp 281–290

Song YS, Hong WP, Woo KS (2012) Behaviour and analysis of stabilizing piles in a cut slope during heavy rainfall. Eng Geol 129–130:56–67. doi:10.1016/j.enggeo.2012.01.012

Zienkiewicz OC, Humpheson C, Lewis RW (1975) Associated and non-associated visco-plasticity in soil mechanics. Geotechnique 25(4):671–689. doi:10.1680/geot.1975.25.4.671

B. Pulko (✉) · B. Majes · M. Mikoš
Faculty of Civil and Geodetic Engineering,
University of Ljubljana,
Jamova cesta 2, SI-1000 Ljubljana, Slovenia
e-mail: bostjan.pulko@guest.arnes.si